

In Vitro Anti-*Propionibacterium* Activity by Curcumin Containing Vesicle System

Chi-Hsien Liu* and Hsin-Ying Huang

Graduate Institute of Biochemical and Biomedical Engineering, Chang Gung University, 259 Wen-Hwa First Road, Kwei-Shan, Tao-Yuan, Taiwan 333, R.O.C.

Received December 5, 2012; accepted January 22, 2013

Propionibacterium acnes acts a critical role in the development of inflammatory acne when it overgrows in pilosebaceous units. The spread of multiple drug resistance bacteria indicates a growing need for new antimicrobial agents. The objective of this study is to develop lipid vehicles to deliver curcumin and inhibit *P. acnes* in the skin. The inhibitory activities of the curcumin containing vehicles against *P. acnes* were studied by the bioluminescence assay. Curcumin accumulation patterns in neonate pig skin were studied using Franz diffusion cells and confocal laser scanning microscopy. The physicochemical properties of the curcumin containing vehicles including interfacial tension, size distribution and viscosity were analyzed. Significant curcumin accumulation ($362 \pm 8 \mu\text{g/g}$ skin) was observed with the lipid vehicles developed herein. Curcumin ($0.43 \mu\text{g/mL}$) in the vehicles significantly inhibited the growth of *P. acnes*. Confocal laser scanning microscopy confirmed the formation of curcumin reservoir in the skin by the curcumin-loaded vehicles. Curcumin-loaded vehicles could efficiently accumulate in the skin and inhibit *P. acnes in vitro*. Our results highlight the potential of using vehicles containing lauric acid and curcumin as an alternative treatment for acne vulgaris.

Key words curcumin; lipid vehicle; *Propionibacterium*; dermal; lauric acid

Propionibacterium acnes, one of the skin commensal bacteria, plays a critical role in the development of inflammatory acne when it overgrows in pilosebaceous units.¹⁾ Inflammatory acne is induced by host immune reactions to *P. acnes*, which releases chemoactive factors that attract the body's immune system cells and stimulates the production of proinflammatory cytokines. Antibiotics are prescribed for acne patients because reduced *P. acnes* numbers correlate with clinical improvement of acne in patients.²⁾ Antibiotics like erythromycin and clindamycin in combination with azelaic acid are used to treat severe acne.³⁾ However, high-dose administration of antibiotics induces the development of multiple-drug resistance and adverse side effects. Therefore, new antimicrobial agents for inhibiting acne bacteria on the skin would be helpful for acne therapy. Plant derivatives like catechol and carnosol can exhibit antibacterial activities against *P. acnes*.^{4,5)} Curcumin extracted from the spice turmeric, has multiple biological activities such as anti-inflammatory, antioxidant, wound-healing and anticancer effects.⁶⁾ Recent studies demonstrated that curcumin loaded alginate foams have antibacterial activity against *Escherichia coli* in photodynamic therapy of infected wounds.⁷⁾ However, few papers reported curcumin's antibacterial activity against *Propionibacterium* species, the main cause of inflammatory acne. Nontraditional antimicrobial agents have garnered tremendous interest in overcoming drug-resistance of pathogenic microorganisms. The effectiveness of antimicrobial nanoparticles and nanosized carriers in treating infectious diseases was proven.⁸⁾ For example, antimicrobial nanoemulsions were found to be effective in killing resistant *Staphylococcus aureus* and *Pseudomonas aeruginosa*.⁹⁾ Essential oil-containing formulation exhibited antimicrobial activity against Gram-negative and Gram-positive bacteria.¹⁰⁾ Recently, fatty acid-loaded liposomes were found to efficiently inhibit *P. acnes* growth by directly fusing into bacterial membranes and releasing the acid cargo.¹¹⁾

Lipid-based vehicle systems such as emulsions and microemulsions are modern colloidal carriers for dermal drug delivery.^{12,13)} Microemulsions are single-phase, optically isotropic nanostructured solutions composed of a surfactant, cosurfactant, oil, and water. Advantages of microemulsion delivery systems include easy preparation, low viscosity, high surface area, high drug solubilization, and optical transparency.¹⁴⁾ Microemulsions were applied to topically deliver different drugs including metronidazole,¹⁵⁾ genistein,¹⁶⁾ chlorogenic acid,¹⁷⁾ and nicardipine.¹⁸⁾ These *in vitro* and *in vivo* studies demonstrated that lipophilic drugs incorporated into microemulsions can efficiently be delivered to the skin. Although topical drug delivery for treating skin disorders is one of the most promising methods, limited research work has focused on curcumin's topical delivery for inhibiting *P. acnes*. The bactericidal properties of lauric acid and curcumin were respectively revealed in two studies.^{7,19)} However, whether curcumin-loaded vehicles can be used to inhibit *P. acnes*, which causes inflammatory acne, has not been demonstrated. High-dose administration of antibiotics induces the development of multiple-drug resistance and adverse side effects. Indeed, a potent drug should be incorporated in stable carriers to inhibit the growth of *P. acnes*. In this study, curcumin was incorporated into vehicles in order to inhibit the growth of *P. acnes*. Moreover, the mechanism of curcumin accumulation in porcine skin was evaluated using neonate pig skin mounted on a Franz diffusion cell and curcumin location in the skin was analyzed by confocal laser scanning microscopy.

Experimental

Materials Curcumin was obtained from Masterasia (Taipei, Taiwan). *P. acnes* BCRC-10723 (ATCC 6919) was obtained from Bioresource Collection and Research Center (Hsinchu, Taiwan) and was cultured on Reinforced Clostridium (RC) medium (Oxoid, Hampshire, England) under anaerobic conditions by using Gas-Pak kit (Becton Dickinson, Sparks, MD, U.S.A.). BacTiter-Glo™ kit for microbial assay

The authors declare no conflict of interest.

* To whom correspondence should be addressed. e-mail: chl@mail.cgu.edu.tw

was purchased from Promega (Madison, WI, U.S.A.). Tween 80, Pluronic F127, isopropanol, and fatty acids were obtained from Sigma (St. Louis, MO, U.S.A.). All reagents were used without further purification. The water used in this study was freshly purified by the Milli-Q Gradient A10 system (Millipore, Molsheim, France).

Preparation of Lipid Vehicles Lauric acid was mixed with isopropanol in the weight ratio of 1:2 to increase its water-solubility. Lipid vehicles composed by lauric acid, isopropanol, and surfactants (Tween 80 and F127) were prepared by drop-wise adding the required amount of water into the pre-mixed solution under gentle magnetic stirring for 10 min. After being equilibrated for 10 min, the systems could form single-phase and transparent lipid systems.

Characterization of Lipid Vehicles Lipid vehicles were prepared by mixing the oil with the surfactant or surfactant/cosurfactant mixture before adding the required amount of water under magnetic stirring. Curcumin (4 g/L) was then added to the prepared vehicles. No phase change was noted after addition of the drug or after equilibration in the water bath. The flow properties and viscosity of the formulations were determined at $32 \pm 1^\circ\text{C}$. Viscosity determinations employed a Brookfield viscometer (DV II+, Brookfield, Stoughton, MA, U.S.A.). Interfacial tension measurements were carried out at room temperature using a thin platinum plate attached to a transducer amplifier (Kyowa CBVP-A3, Saitama, Japan). During the measurement, the plate is dipped into the tested vehicles. The tensiometer measures the pulling force of the liquid on the plate and calculates the interfacial tension by dividing by the known plate size. The average particle size was characterized using a Zetasizer Nano ZS 90 (Malvern, Worcestershire, U.K.) at a fixed angle of 90° and a temperature of 32°C . Lipid vehicles were measured without dilution by water or solvent in order to avoid the dilution effects on the size distribution of the vehicles.

In Vitro Curcumin Dermal Accumulation Full-thickness skin from the pig ear is a generally accepted model of permeation for human dermatological research.²⁰ The skin of the outside of the ears of corpses of new-born piglets was used to study the permeation of curcumin in a Franz diffusion assembly. The ear skin was mounted between the donor and receptor compartments with the stratum corneum side facing the donor compartment. The donor medium consisted of 0.5 mL of vehicle containing curcumin. The receptor medium (5.5 mL) was obtained by mixing 1:1 ethanol and phosphate-buffered saline (PBS, pH 7.4) in order to maintain sink conditions. Similar solution was successfully applied to monitor the skin delivery of curcumin from microemulsions.²¹ The available diffusion area between the cells was 0.785 cm^2 . The stirring rate and temperature were respectively kept at 600 rpm and 32°C . At appropriate intervals, all receptor medium was withdrawn and immediately replaced with equal volumes of fresh medium. Cumulative amount of curcumin permeated after 24 h diffusion was used to calculate the transdermal drug flux. The permeated amount of curcumin was determined by high-performance liquid chromatography (HPLC). A skin sample with the 0.785 cm^2 permeated area was cut, weighed, and then homogenized in a 50% ethanol PBS solution for 5 min at a 10000 rpm rate. The resulting solution was centrifuged, and the supernatant was analyzed by HPLC. Quantification of curcumin was achieved using an HPLC system (Jasco, Tokyo,

Japan) consisting of a pump, a UV detector, and a Microsorb-C18 column (Varian, Lake Forest, CA, U.S.A.). The mobile phase was consisted of 1% (w/v) acetic acid, 73% (w/v) methanol, and 26% (w/v) water. The flow rate of the mobile phase was 1.0 mL/min and the column effluent was monitored at 430 nm.

Inhibitory Activity of Lipid Vehicles against *P. acnes* Single colony of *P. acnes* was inoculated in RC medium and cultured at 37°C until reaching around OD_{600} 1.0 (logarithmic growth phase) under anaerobic conditions. Then the seed culture was diluted with fresh RC medium to the value of 0.1 (OD_{600}) for further microbial growth experiments. Drugs and fatty acid-contained vehicles were diluted by dimethyl sulfoxide (DMSO) in a 2-fold serial manner and added at the 1% volume ratio to the 96-well microtiter plates. The bacteria were cultured in plates (volume = 0.2 mL) for 24 h and the growth was quantified by measuring the absorbance at OD_{600} . When the curcumin was added in the formulations, the bacterial growth was quantified by the BacTiter-Glo™ kit (Promega) to avoid the interference of curcumin color at OD_{600} . The kit uses bioluminescence produced by luciferase to detect the intracellular concentration of ATP, which correlates with viable bacterial cell numbers.²² In brief, the reaction involves adding a single reagent directly to bacterial cells cultured in medium and measuring luminescence generated by bacterial ATP and a thermostable luciferase. The bioluminescence was measured by Epoch Spectrophotometer H4 (Biotek, Winooski, VT, U.S.A.). The control group was *P. acnes* incubated with 1% (v/v) DMSO. The growth inhibition at OD_{600} can be determined from the following equation:

$$\text{inhibition} = [1 - (\text{absorbance}_{\text{treatment}} / \text{absorbance}_{\text{control}})] \times 100\%$$

Confocal and Histological Examination of Porcine Skin Porcine skin samples obtained from the diffusion device were fixed in PBS solution containing 10% formalin. Sequentially skin was dehydrated using ethanol, embedded in paraffin, sectioned longitudinally by microtome (Leica RM 2235, Bannockburn, IL, U.S.A.) at $5\text{ }\mu\text{m}$ thickness, and finally stained with hematoxylin eosin (HE) staining. These section samples were then observed under light microscope (Olympus BX51, Tokyo, Japan) using $40\times$ magnification. For observation by confocal laser scanning microscopy (CLSM), the skin was removed from the diffusion cell and directly observed without wiping the curcumin on skin surface with the ethanol solution. The skin sample was sandwiched between a glass slide and a coverslip in a 1:1 solution of PBS-glycerol, and examined confocal microscopy without additional processing. Fluorescent images were obtained by Leica TCS SP2 confocal laser scanning microscope (Leica, Nidau, Switzerland). The fluorescence of curcumin was excited at a wavelength of 420 nm by means of an argon laser. To visualize the distribution of curcumin, confocal images were first obtained in the xy -plane. The top surface of skin ($z=0\text{ }\mu\text{m}$) was defined as the fluorescence plane with a morphology characteristic of the stratum corneum surface. To generate an xz -section, a horizontal line was “drawn” across a region of interest in the $z=0\text{ }\mu\text{m}$ - xy -plane and then “optically sliced” through the digitized image data of the successive xy -sections to generate xz -planar optical cross-sections. The skin sample was scanned from the skin surface ($0\text{ }\mu\text{m}$) to a depth of $160\text{ }\mu\text{m}$ at a $10\text{-}\mu\text{m}$ interval. All images were the average of four scans and the data were

obtained with the same optical aperture, lens and scan speed.

Results and Discussion

Inhibition of Fatty Acids, Azelaic Acid and Curcumin against *P. acnes* The inhibitory effects of fatty acids with different chain lengths on *P. acnes* are investigated herein to evaluate their antimicrobial effects (Table 1). The fatty acids tested in this study included butyric, caproic, aminocaproic, heptanoic, octanoic, decanoic, lauric, myristic, palmitic, and stearic acids. Middle-chain fatty acids such as decanoic, lauric, myristic and palmitic acids significantly inhibited the growth of *P. acnes* ($p < 0.05$) at the concentration of $50 \mu\text{g/mL}$. The inhibition efficacy was ranked in the following order: lauric > myristic > decanoic > palmitic acid (Table 1). The short-chain fatty acids (carbon number < 8) and stearic acid only slightly inhibited the growth of *P. acnes*. Among the tested fatty acids, lauric acid most effectively inhibited the growth of *P. acnes*. Azelaic acid (a nonanedioic acid) was chosen as a control, since it was approved for treating mild-to-moderate acne vulgaris.³⁾ The dose effects of curcumin, azelaic acid, and lauric acid on *in vitro* inhibition of *P. acnes* were evaluated (Fig. 1). Curcumin and lauric acid strongly inhibited microbial growth compared to azelaic acid. Their inhibition abilities were ranked in the order of curcumin > lauric acid > azelaic acid with respective 50% inhibitory concentrations (IC_{50}) of 23.7, 25.0, and $847.6 \mu\text{g/mL}$. Notably, there was a 36-fold drop in the IC_{50} concentration for curcumin compared to azelaic acid. Lauric acid also had a 34-fold increase in inhibition compared to azelaic acid. Since the water solubility of lauric acid is only $3.4 \mu\text{g/g}$, the inhibitory effect of lauric acid against *P. acnes* was limited after the concentration of lauric acid reached $31.25 \mu\text{g/mL}$ (Fig. 1). When lauric acid added at high concentrations, it formed the oil film with limited surfaces for lauric acid dissolution. Therefore, the low solubility results in a decreased potency for *P. acnes* inhibition. Our results indicated the potency of curcumin and lauric acid as candidates for inhibiting *P. acnes*. Azelaic acid, the ingredient of commercial therapeutics, showed the least antimicrobial activity against *P. acnes*. However, curcumin and lauric acid are both hydrophobic which limits their delivery route and availability. New lipid vehicles will be developed for transdermal delivery of curcumin and lauric acid in the next section.

Composition Effects on Dermal Curcumin Accumulation Emulsions are composed of an aqueous phase, an oil phase, and surfactant/cosurfactant. Since lauric acid is a saturated fatty acid with limited water solubility ($3.4 \mu\text{g/g}$ water), isopropanol can act as a cosurfactant to increase the solubility of lauric acid and enhance the stability of the oil–water interface. Lauric acid was the oil phase in the system that used to accommodate curcumin with Tween 80, isopropanol as the surfactants and cosurfactant, respectively. The lauric acid/isopropanol mass ratio was fixed at 1:2. In order to evaluate the formula effects, the abilities of eighteen vehicles to deliver curcumin and its accumulation in a porcine skin model were tested. The compositions of LM1–LM6 are shown in Table 2. The curcumin accumulation in the skin increased from 0.1 to $208 \mu\text{g/g}$ skin as the Tween 80 content decreased (Fig. 2). The vehicles (LM4–LM6) with low surfactant/water ratio could enhance curcumin accumulation and penetration in porcine skin model herein. Maximal curcumin accumulated in the skin was observed with the vehicle (LM6+5%F127) composed

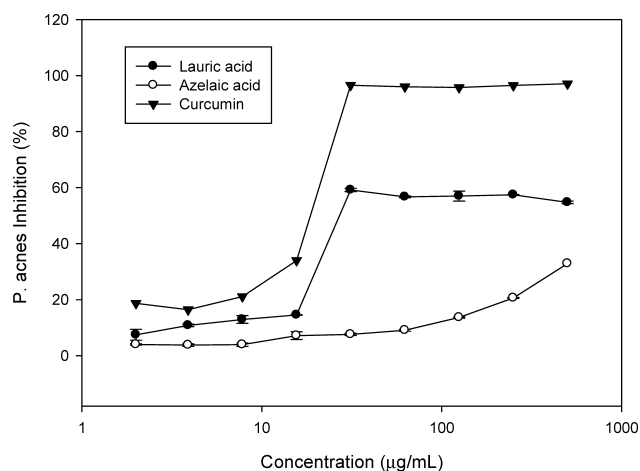


Fig. 1. Inhibition Profiles of *P. acnes* by Lauric Acid, Azelaic Acid, and Curcumin

The concentration range of the tested compounds is 2–500 $\mu\text{g/mL}$ by using DMSO as the vehicle. The error bar stands for standard deviation ($n=3$).

Table 1. Inhibition of Various Fatty Acids on *P. acnes*^{a)}

Fatty acids	<i>P. acnes</i>
	Inhibition (%)
Sodium butyrate (C4)	2.03 ± 0.24
Caproic acid (C6)	2.92 ± 0.63
Heptanoic acid (C7)	1.00 ± 0.74
Octanoic acid (C8)	1.00 ± 0.48
Decanoic acid (C10)	30.63 ± 0.01
Lauric acid (C12)	67.80 ± 0.72
Myristic acid (C14)	35.90 ± 0.39
Palmitic acid (C16)	9.86 ± 0.90
Stearic acid (C18)	1.00 ± 0.48

a) The tested concentration for various fatty acids was $50 \mu\text{g/mL}$ by using DMSO as the solvent. The results represents average \pm S.D. ($n=3$).

of 5% F127, 31.6% isopropanol, 15.9% lauric acid, and 47.5% water. Microemulsion is defined as single-phase solutions composed of surfactant, cosurfactant, oil, and water.¹⁴⁾ LM6 (containing lauric acid, isopropanol and water) is not a microemulsion since no surfactant exists. Hence, 5% F127 was incorporated in lauric acid formulations (LM1–LM6) to elevate their performance in this study (Table 1, and Figs. 2–6). Our results indicated that LM6+5%F127 had the maximal curcumin accumulation compared to formulations (LM1–LM6) without F127 addition. Besides, the addition of 5% F127 reduced the colloidal sizes of LM6 from 246 (0% F127) to 151 nm and helped the LM6 stable. Although Tween 80 could stabilize the lipid vehicles and minimize the droplet size, the curcumin accumulation in the skin decreased as Tween 80 content increased (Fig. 2). The objective of this study was to develop lipid vehicles for curcumin accumulation on the topical skin, the LM6+5%F127 was chosen and characterized elaborately. Better curcumin accumulation in skin was observed when comparing LM6+5%F127 with LM6. F127 incorporated into vehicles could increase the delivery efficacy as shown in Fig. 2. The good solubility, low toxicity, and sustained release characteristics of F127 render it an attractive candidate as a pharmaceutical vehicle for drugs.²³⁾ For example, F127 was used to enhance the delivery of 5-aminolevulinic acid for treating actinic keratosis in photodynamic therapy.²⁴⁾ F127

combined with lecithin enhanced the stability and absorption of sumatriptan across the skin.²⁵⁾ Percutaneous absorption of nonivamide from F127 vehicles was reported by using Wistar rats as an animal model.²⁶⁾ Here, 5% F127 combined with lauric acid vehicles (LM1–LM6) elevated curcumin accumulation compared to vehicles without F127 addition. However, a higher F127 content (10%) did not enhance curcumin accumulation in the skin compared to the control (0%) and 5% F127 supplement. Maximal effects of 5% F127 on curcumin dermal accumulation were observed as indicated in Fig. 2. It was noted that hydration by water in the stratum corneum can enhance drug delivery as previously described.²⁷⁾ LM6 had the highest water content (50%) compared to the LM1–LM5. The curcumin accumulation in the skin by the vehicles of LM6, LM6+5%F127 and LM6+10%F127 were 207.8, 362.1 and 89.9 $\mu\text{g/g}$ skin, respectively (Fig. 2). We found that the addition of 5% F127 to LM6 enhanced curcumin's topical accumulation in porcine skin. The drug accumulated in the stratum corneum might form a reservoir, sustain the drug release and inhibit the growth of *P. acnes*. Sequentially, the antimicrobial activities of the vehicles (LM6 vs. LM6+5%F127) were analyzed in the next section.

Inhibition of *P. acnes* by Curcumin Vehicles The antimicrobial activities of the curcumin-loaded lauric acid vehicles and curcumin/lauric acid mixture were investigated to evaluate their inhibition effects. Curcumin-loaded vehicles and curcumin/lauric acid were serially diluted and incubated with *P. acnes* in RC medium for 24 h to determine their luminescence intensities (*i.e.* growth condition). The results indicated that 0.43 $\mu\text{g/mL}$ curcumin in the vehicle (containing 17.2 $\mu\text{g/mL}$ lauric acid) inhibited 50% bacterial growth. The addition of 5% F127 to the lipid vehicle did not affect the antimicrobial activity compared to the LM6 (Fig. 3). In contrast, the mixture of curcumin and lauric acid in DMSO inhibited 50% growth of *P. acnes* at high concentrations (both 11.9 $\mu\text{g/mL}$). From these results, the antimicrobial activity of curcumin-loaded vehicles could be confirmed. Previously 80 $\mu\text{g/mL}$ lauric acid in a liposome vehicle could inhibit the growth of *P. acnes*.¹¹⁾ The antimicrobial activity of curcumin was significantly enhanced by loading it in lauric acid vehicles herein. Our data showed that curcumin-loaded vehicles were more effective than curcumin or lauric acid alone in inhibiting the growth of *P. acnes* (Figs. 1, 3). The possible mechanisms for the enhanced effectiveness of lauric acid vehicles might be due to the following reasons. Nanosized vehicles can help drugs (lauric acid and curcumin) contact with bacteria and efficiently penetrate the cell membranes. Previously, the *in vitro* antimicrobial activity of azelaic acid against *P. acnes* strain

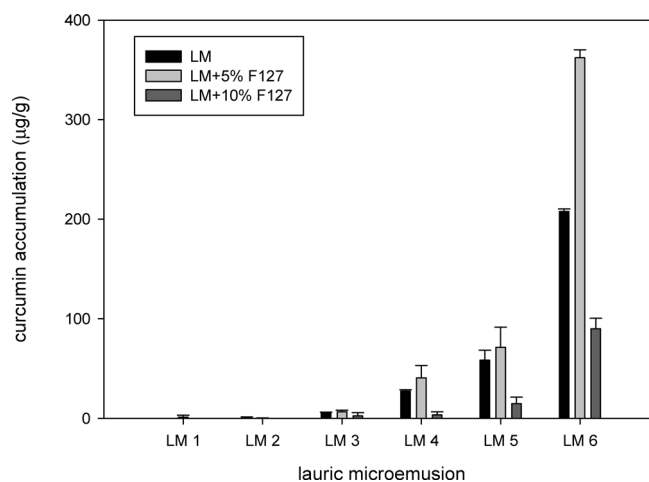


Fig. 2. Ingredient Effects of Vehicle on Curcumin (0.4%, w/v) Accumulation in Porcine Skin

The detailed composition of vehicles is listed in Table 1. The error bar stands for standard deviation ($n=3$).

P37 was studied. At a concentration of 500 mM (94.1 mg/mL), azelaic acid exhibited bactericidal activity, while the addition of nutrients reduced bacterial susceptibility.²⁸⁾ In contrast, curcumin inhibited 96.5% of the growth of *P. acnes* at 31.2 $\mu\text{g/mL}$ concentration. Therefore curcumin showed much greater inhibitory ability against *P. acnes* compared to lauric acid. In recent years, Yang *et al.* found the minimal inhibition concentration of lauric acid to be about 65 $\mu\text{g/mL}$ by a colony-forming method.¹¹⁾ We found that lauric acid alone could inhibit 59.2% of *P. acnes* growth at a concentration of 31.2 $\mu\text{g/mL}$ (Fig. 1). Combination of curcumin and lauric acid in the lipid vehicle exhibited strong inhibition against *P. acnes* at 0.43 $\mu\text{g/mL}$ curcumin and 17.2 $\mu\text{g/mL}$ lauric acid. Curcumin and its derivatives exhibited antibacterial activity against *Sta. aureus*, *E. coli*, *Bacillus cereus*, and *Yersinia enterocolitica*.²⁹⁾ The antibacterial activity of curcumin is due to inhibition of the cytokinetic Z-ring assembly from FtsZ protofilaments. The Z-ring assembly plays critical roles in bacterial cytokinesis.³⁰⁾ Additionally, lauric acid inhibits Gram-positive cocci by disintegrating the cell membrane, resulting in cytoplasmic disorganization of the bacteria.¹⁹⁾ Combined treatment with two agents possessing distinct mechanisms may exert a more-potent inhibitory effect than a single agent. For example, the combination of 5% azelaic acid and 2% clindamycin is used to clinically treat acne vulgaris.³⁾ Our aim was to develop lauric acid vehicles to deliver curcumin to the skin in order to inhibit *P. acnes*. Only 0.43 $\mu\text{g/mL}$ curcumin loaded in the

Table 2. Composition and Particular Size for Vehicle Formula^{a)}

	Composition				Particular size (nm)		
	Tween 80	Water	Lauric acid	IPA	LM	LM (95%) +F127 (5%)	LM (90%) +F127 (10%)
LM1	50	0	16.7	33.3	6.8±1.2	1.5±0.8	2.6±0.4
LM2	40	10	16.7	33.3	3.6±0.6	2.1±0.8	1.8±0.9
LM3	30	20	16.7	33.3	4.0±0.8	3.7±1.2	129.5±12.0
LM4	20	30	16.7	33.3	16.7±0.7	17.0±1.2	37.2±8.0
LM5	10	40	16.7	33.3	27.3±2.3	275.8±5.8	71.0±31.9
LM6	0	50	16.7	33.3	246.3±18	151.7±4.7	51.2±6.2

a) The particular size was measured after one-week storage at room temperature. The results represents average ±S.D. ($n=3$).

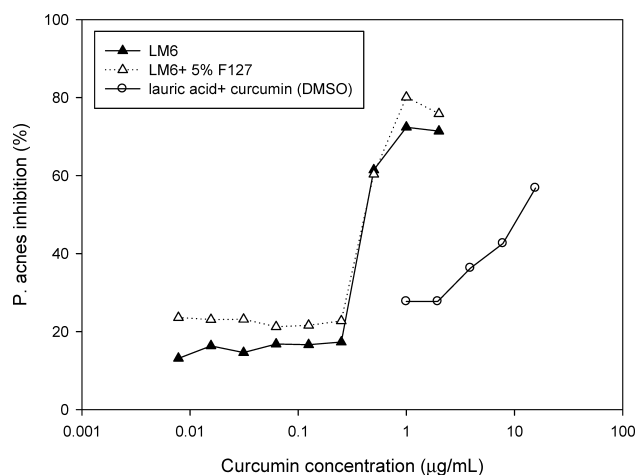


Fig. 3. Inhibition of Curcumin in Various Vehicles on *P. acnes*

The concentration range of curcumin is 0.0078–8.0 µg/mL using DMSO as the solvent. The vehicles (LM6 and LM6+5%F127, both containing 4 mg/mL curcumin) were 500-fold diluted by DMSO and the diluted stocks were used for the antimicrobial experiments. LM6 stock containing 8 µg/mL curcumin and 334 µg/mL myristic acid was diluted in a 2-fold serial manner for the anti-*P. acnes* experiments. Similarly, LM6+5%F127 stock containing 8 µg/mL curcumin and 317 µg/mL myristic acid was serially diluted to 0.0078 µg/mL curcumin and 0.31 µg/mL myristic acid, respectively. The error bar stands for standard deviation ($n=3$).

developed vehicle achieved 50% microbial inhibition, which required 11.9 µg/mL of curcumin by itself as indicated in Figs. 1 and 3. Our *in vitro* results indicate that the cocktail combination of lauric acid and curcumin in the vehicle carrier might provide a new strategy for anti-*P. acnes* therapy. In order to understand the curcumin distribution after applied to the skin, confocal laser scanning microscopy (CLSM) was used to recorder the passage of curcumin in the next section.

Curcumin Distribution in Skin and Histological Staining CLSM is extensively used as a tool to visualize fluorescent model compounds in skin.³¹⁾ This method does not require fixation of skin samples and thereby reduces the redistribution of the stain and tissue damage. The fluorescence of curcumin could be applied to trace its transdermal route using excitation at 430 nm and emission at 540 nm. Figure 4 presents curcumin distribution in the skin with three different vehicles of PBS, LM6, and LM6+5%F127 by using CLSM. The fluorescence intensities of curcumin in the skin were ranked LM6+5%F127 > LM6 > PBS. These results are consistent with curcumin accumulation in the Franz cell-diffusion experiments (Fig. 2). Curcumin's distribution at different skin depths could be visualized in Fig. 4. The total path length of fluorescence observation was 160 µm using the stratum corneum as 0 µm. Curcumin distribution in the skin was observed for the three tested formulations under occlusion conditions. The fluorescence intensity of curcumin in three vehicles (PBS, LM6 or LM6+5%F127) at the porcine skin were directly observed without using ethanol to clean the skin surface. The ethanol wipe might extract curcumin from the skin and mislead the penetration results. The fluorescence intensity of CLSM images showed that LM6+5%F127 formulation exhibited the strongest intensity of curcumin at the epidermis layer which provided a driving force for further curcumin penetration. Slight curcumin penetration from PBS was observed at 25 µm depth. In contrast, curcumin could penetrate to the skin depth of 65 µm with the help of LM6+5%F127 vehicle. However, deep skin (>70 µm) showed little fluorescence for

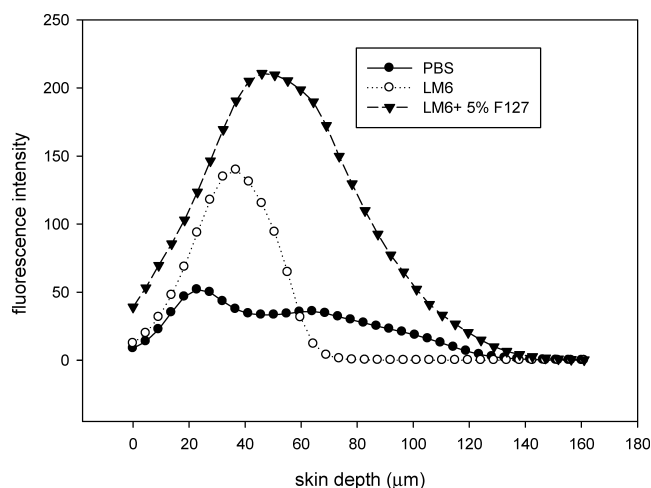


Fig. 4. Distribution of Curcumin in Porcine Skin after 24h Diffusion by Using Confocal Laser Scanning Microscopy

Three vehicles contain 0.4% (w/v) curcumin including PBS (A), LM6 (B), and LM6+5% F127 (C). HeNe laser was used to excite curcumin at 430 nm with emission fluorescence at 540 nm. Thirty photos (from left to right, 6×5) were scanned from the skin surface (0 µm) to a depth of 160 µm at a 10-µm interval. All samples contain 0.4% (w/v) curcumin.

three vehicles which might be due to tissue absorption and light scatter. The CLSM results of the present study showed penetration profiles of curcumin within the skin were dependent on vehicle compositions. The fluorescence intensity of curcumin in skin (Fig. 4) also confirmed the conclusion of the diffusion experiment that LM6+5%F127 could enhance the accumulation in porcine skin.

The safety of transdermal delivery vehicles is important for formulation development. Histological safety for treated (LM6+5% F127) and control (PBS) skin was performed using light microscopy to investigate skin changes after H&E staining. Micrographs of control and treated samples demonstrated similar skin layers as shown in Figs. 5A and B. Normal morphology of the SC was observed in skin treated with vehicle or PBS. No apparent epidermal changes were observed in the two samples. A photograph of the skin sample with 24-h vehicle treatment showed a thin keratin layer, a normal dermis, and subcutaneous tissues. Keratin fragmentation and disruption of the lipid bilayers were observed in skin treated with the vehicle for 24 h. Ablation of the SC may have contributed to the enhancing effect of the vehicles on curcumin permeation. A photograph of the control skin sample showed a similar SC (arrow in Fig. 5) as skin treated with LM6+5% F127. No significant changes were observed in histological photos of vehicle-treated skin and control skin. Some areas of the skin (both LM6-treated) had empty spaces in the dermal region. These empty spaces could help the *in vitro* curcumin accumulation in the skin. However, more *in vivo* tests are needed in order to evaluate whether the developed vehicle is safe for inhibition of *P. acnes* on the skin.

Characterization of Lipid Vehicles Colloid size is one of the important physicochemical properties impacting the stability, biodistribution, and release kinetics of lipid vehicles. Size distributions of the vehicles developed are shown in Table 2. The particle size of these 18 emulsions was <276 nm and could be classified as emulsions according to the definition by Shah *et al.*³²⁾ The addition of F127 reduced the colloidal sizes of LM6 from 246 (0% F127) to 51 nm (10% F127). Particle

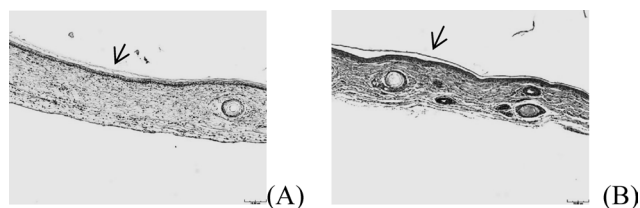


Fig. 5. Micrographs of HE Staining after 24-h Treatment with Formulations: PBS (A) and LM6 +5% F127 (B)

Arrow indicates the stratum corneum. Scale bar represents 10 μ m. All samples contain 0.4% (w/v) curcumin.

sizes of the emulsions decreased as the surfactant in the formulation increased. Surfactants can reduce the colloidal size by reducing the surface tension and fluidizing the interfacial droplet film.³³⁾ However, a small colloid size did not ensure high curcumin penetration or skin accumulation as determined by comparing LM1 (with a 6-nm diameter) with LM6 (with a 246-nm diameter). LM6+5% F127 with a 152-nm diameter had the best curcumin accumulation in porcine skin among the formulations tested. The characteristics of surface tension and viscosity are used to describe the colloidal properties of emulsions.³⁴⁾ In this study, the viscosity and surface tension of curcumin-loaded emulsions were summarized in Fig. 6. The surface tension of vehicles slightly changed from 24 to 26 mN/m when the F127 or water contents increased. The surface tension of the tested vehicles was low compared to the surface tension of water (72.0 mN/m). The viscosity of curcumin-loaded vehicles was also analyzed. The viscosity of vehicles increased from 24.9 to 60.1 cP when F127 increased from 0% to 10% (Fig. 6). The viscosity slightly decreased, and then increased when the water content reached 50% for all vehicles.

The ratio of surfactant/water in LM1–LM6 (Table 2) significantly influenced curcumin accumulation in porcine skin (Fig. 2). The following reasons might contribute to the enhancing accumulation effects under high water-content conditions. Similar increasing of domperidone delivery was observed in skin when decreasing Tween 20 concentration.³⁵⁾

Microemulsion structure (water-in-oil or oil-in-water) also affects the delivery efficacy of drug.¹⁴⁾ Emulsions would change from water-in-oil to oil-in-water types when the water content increased. The surface tension of all tested vehicles was very low (around 24–26 mN/m) which is the characteristic of vehicle. The low surface tension of these vehicles may facilitate formation of nanosized colloids in suspension which prevents the phase separation and maintains the stability. Additionally low surface tension may help the contact of lipid vehicles with the skin and enhance the curcumin accumulation in the skin.¹⁴⁾ The viscosity of drug-loaded vehicles was reported to influence drug partitioning into the skin. High viscosity hampers the efficacy of transdermal delivery as it decreases the diffusion rate.³⁶⁾ Others reasons could be proposed to explain the enhancing effects of LM6+5%F127 on curcumin accumulation in the skin. For example, ingredients of vehicle adsorbed in the skin may modulate the stratum corneum and increase the partitioning of curcumin into the skin. This curcumin reservoir could create a high drug concentration within the upper layers of the skin and result in a high curcumin gradient as a driving force for transdermal curcumin delivery. This possibility was supported by our CLSM results that efficient delivery of curcumin was accompanied by high curcumin retention in the skin. Another possibility is that lauric acid is a well-known skin penetration enhancer which disturbs the double layers of the epidermis.³⁷⁾

Conclusion

We successfully developed lipid vehicles to deliver curcumin to the skin for *P. acnes* inhibition. Combined effects of curcumin and lauric acid were found in inhibiting *P. acnes*. The delivery route of curcumin in porcine skin was confirmed by confocal laser scanning microscopy. The anti-*Propionibacterium* activity of curcumin and lauric acid was significantly enhanced by the nanosized vehicle. A histological examination confirmed normal skin morphologies after lipid vehicle treatments. In summary, curcumin-loaded vehicles are a promising tool for the topical delivery of curcumin to inhibit the growth of *P. acnes*.

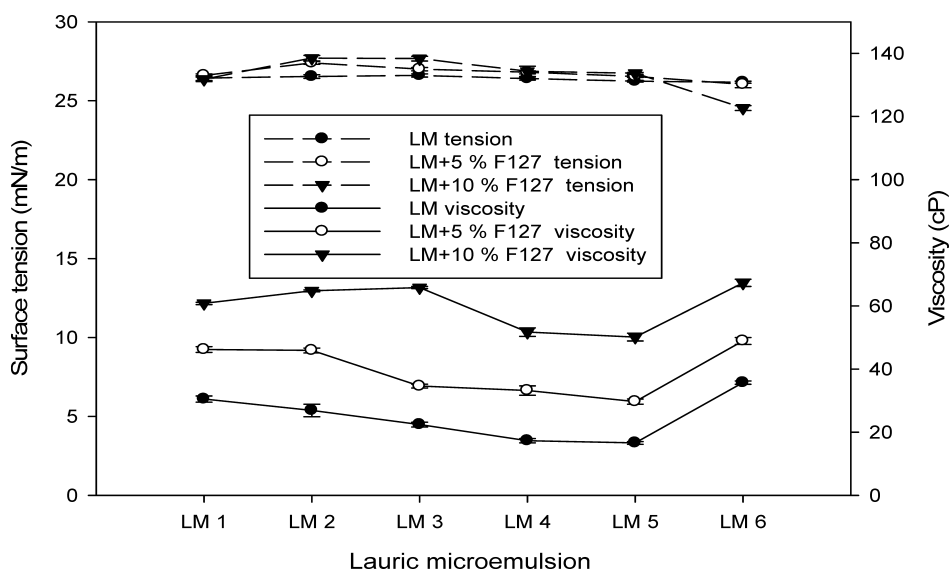


Fig. 6. Characterization of Surface Tension and Viscosity for Vehicles Containing 0.4% (w/v) Curcumin

The detailed composition of vehicles is listed in Table 1. The error bar stands for standard deviation ($n=3$).

Acknowledgments The project was kindly supported by National Science Council (NSC 101-2628-E-182-001) and Chang Gung Memorial Hospital (CMRPD 2A0101), Taiwan.

References

- 1) Brüggemann H., Henne A., Hoster F., Liesegang H., Wiezer A., Strittmatter A., Hujer S., Dürre P., Gottschalk G., *Science*, **305**, 671–673 (2004).
- 2) Chia H. Y., Tey H. L., Lee J. S. S., *J. Dermatol.*, **38**, 409–411 (2011).
- 3) Pazoki-Toroudi H., Nassiri-Kashani M., Tabatabaie H., Ajami M., Habibey R., Shizarpour M., Babakoochi S., Rahshenas M., Firooz A., *J. Dermatolog. Treat.*, **21**, 212–216 (2010).
- 4) Tada M., Ohkanda T., Kurabe J., *Chem. Pharm. Bull.*, **58**, 27–29 (2010).
- 5) Tada M., Kurabe J., Yoshida T., Ohkanda T., Matsumoto Y., *Chem. Pharm. Bull.*, **58**, 818–824 (2010).
- 6) Chaudhary H., Kohli K., Amin S., Rathee P., Kumar V., *J. Pharm. Sci.*, **100**, 580–593 (2011).
- 7) Hegge A. B., Andersen T., Melvik J. E., Kristensen S., Tønnesen H. H., *J. Pharm. Sci.*, **99**, 3499–3513 (2010).
- 8) Huh A. J., Kwon Y. J., *J. Controlled Release*, **156**, 128–145 (2011).
- 9) Teixeira P. C., Leite G. M., Domingues R. J., Silva J., Gibbs P. A., Ferreira J. P., *Int. J. Food Microbiol.*, **118**, 15–19 (2007).
- 10) Pérez-Vásquez A., Capella S., Linares E., Bye R., Angeles-López G., Mata R., *J. Pharm. Pharmacol.*, **63**, 579–586 (2011).
- 11) Yang D., Pornpattananangkul D., Nakatsuji T., Chan M., Carson D., Huang C. M., Zhang L., *Biomaterials*, **30**, 6035–6040 (2009).
- 12) Chao Y., Huang C. T., Fu L. T., Huang Y. B., Tsai Y. H., Wu P. C., *Chem. Pharm. Bull.*, **60**, 1171–1175 (2012).
- 13) Liu C. H., Chang F. Y., *Chem. Pharm. Bull.*, **59**, 172–178 (2011).
- 14) Spornath A., Aserin A., *Adv. Colloid Interface Sci.*, **128–130**, 47–64 (2006).
- 15) Tirnaksiz F., Kayış A., Çelebi N., Adışen E., Erel A., *Chem. Pharm. Bull.*, **60**, 583–592 (2012).
- 16) Kitagawa S., Inoue K., Teraoka R., Morita S. Y., *Chem. Pharm. Bull.*, **58**, 398–401 (2010).
- 17) Kitagawa S., Yoshii K., Morita S. Y., Teraoka R., *Chem. Pharm. Bull.*, **59**, 793–796 (2011).
- 18) Wu P. C., Lin Y. H., Chang J. S., Huang Y. B., Tsai Y. H., *Drug Dev. Ind. Pharm.*, **36**, 1398–1403 (2010).
- 19) Desbois A. P., Smith V. J., *Appl. Microbiol. Biotechnol.*, **85**, 1629–1642 (2010).
- 20) Sekkat N., Kalia Y. N., Guy R. H., *Pharm. Res.*, **21**, 1390–1397 (2004).
- 21) Liu C. H., Chang F. Y., Hung D. K., *Colloids Surf. B Biointerfaces*, **82**, 63–70 (2011).
- 22) Sule P., Wadhawan T., Carr N. J., Horne S. M., Wolfe A. J., Prüss B. M., *Lett. Appl. Microbiol.*, **49**, 299–304 (2009).
- 23) Escobar-Chávez J. J., López-Cervantes M., Naik A., Kalia Y. N., Quintanar-Guerrero D., Ganem-Quintanar A., *J. Pharm. Pharm. Sci.*, **9**, 339–358 (2006).
- 24) Grüning N., Müller-Goymann C. C., *J. Pharm. Sci.*, **97**, 2311–2323 (2008).
- 25) Agrawal V., Gupta V., Ramteke S., Trivedi P., *AAPS PharmSciTech*, **11**, 1718–1725 (2010).
- 26) Fang J. Y., Leu Y. L., Wang Y. Y., Tsai Y. H., *Eur. J. Pharm. Sci.*, **15**, 417–423 (2002).
- 27) Narishetty S. T. K., Panchagnula R., *J. Controlled Release*, **102**, 59–70 (2005).
- 28) Bojar R. A., Holland K. T., Cunliffe W. J., *J. Antimicrob. Chemother.*, **28**, 843–853 (1991).
- 29) Parvathy K. S., Negi P. S., Srinivas P., *Food Chem.*, **115**, 265–271 (2009).
- 30) Rai D., Singh J. K., Roy N., Panda D., *Biochem. J.*, **410**, 147–155 (2008).
- 31) Verma D. D., Verma S., Blume G., Fahr A., *Eur. J. Pharm. Biopharm.*, **55**, 271–277 (2003).
- 32) Shah P., Bhalodia D., Shelat P., *Systematic Reviews in Pharmacy*, **1**, 24–32 (2010).
- 33) Garti N., Yagmur A., Leser M. E., Clement V., Watzke H. J., *J. Agric. Food Chem.*, **49**, 2552–2562 (2001).
- 34) Fan Y., Simon S., Sjöblom J., *Colloids Surf. A Physicochem. Eng. Asp.*, **366**, 120–128 (2010).
- 35) Akhter S., Jain G. K., Ahmad F. J., Khar R. K., Jain N., Khan Z. I., Talegaonkar S., *Current Nanoscience*, **4**, 381–390 (2008).
- 36) Liu H., Li S., Wang Y., Han F., Dong Y., *Drug Dev. Ind. Pharm.*, **32**, 549–557 (2006).
- 37) Azeem A., Khan Z. I., Aqil M., Ahmad F. J., Khar R. K., Talegaonkar S., *Drug Dev. Ind. Pharm.*, **35**, 525–547 (2009).